Journal of Luminescence 135 (2013) 74–78

Contents lists available at SciVerse ScienceDirect

Journal of Luminescence

journal homepage: www.elsevier.com/locate/jlumin

Crystal field calculations of energy levels of the Ni^{2+} ions in MgO

N. Mironova-Ulmane [a], M.G. Brik [b,*], I. Sildos [b]

[a] Institute of Solid State Physics, University of Latvia, Kengaraga street 8, LV-1063, Riga, Latvia
[b] Institute of Physics, University of Tartu, Riia 142, Tartu 51014, Estonia

ARTICLE INFO

Article history:
Received 23 May 2012
Received in revised form
17 September 2012
Accepted 19 October 2012
Available online 27 October 2012

Keywords:
Crystal field theory
Spin-orbit splitting
Ni^{2+} ions.

ABSTRACT

The electronic energy levels of six-fold coordinated Ni^{2+} ion in magnesium oxide MgO were calculated using the exchange charge model of crystal field theory. The calculated energetic positions of the Ni^{2+} levels match well the experimental spectrum. Inclusion of the spin-orbit (SO) interaction is compulsory to account for the first excited $^3T_{2g}$ state fine structure; however, it does not explain why out of four levels arising from the $^3T_{2g}$ state, only two are seen in the experimental spectra. One possible explanation to this fact can be advanced by invoking the Jahn–Teller effect.

1. Introduction

Magnesium oxide MgO doped with divalent nickel ions is a classical system to study the energy levels of the $3d^8$ electron configuration in a weak octahedral crystal field (CF). Spectroscopic properties of this material have been analyzed in fine details starting from 1960 s onward [e.g. 1–14]. Such an interest to this system was to a large extent driven by a possibility of getting tunable laser generation in the infrared spectral region, based on the $^3T_{2g}$ –$^3A_{2g}$ emission transition of Ni^{2+}, which, in addition, is only weakly dependent on temperature due to its magnetic dipole nature. By now there has been in principle reached a firm agreement on how the energy levels of divalent nickel ions are positioned in MgO, although some details of the fine structure of the experimental spectra are still a matter of debate.

Fig. 1 shows the Tanabe–Sugano diagram for the Ni^{2+} ions in an octahedral CF. In practically all cases Ni^{2+} ions are located at the crystal lattice sites with a weak CF. The overall absorption spectrum of MgO:Ni^{2+} is determined by three wide bands corresponding to the spin-allowed transitions from the $^3A_{2g}$ ground state to the $^3T_{2g}$, $^3T_{1g}(^3F)$, and $^3T_{1g}(^3P)$ states at about 8000 cm^{-1}, 15,000 cm^{-1}, and 24000 cm^{-1}, correspondingly (Fig. 2). The lowest in energy $^3A_{2g}$ - $^3T_{2g}$ absorption transition is magnetic dipole allowed. These most prominent absorption bands have some superimposed structure, which is caused by the low-intensity spin-forbidden transitions from the $^3A_{2g}$ ground spin-triplet state to the excited spin-singlet states.

However, it should be emphasized that in spite of considerable amount of publications on this subject still there exists a certain controversy regarding an interpretation of the fine structure of the Ni^{2+} first excited $^3T_{2g}$ state in MgO. One point of view is to explain two observed absorption peaks at about 8000 cm^{-1} and 8180 cm^{-1} as the transitions from the ground $^3A_{2g}$ (T_2) state to two lower E, T_1 spin-orbit (SO) split states originating from the $^3T_{2g}$ level [3]. At the same time, two remaining SO split components T_2, A_2 are not observed in the absorption spectra at all. An essential point here is that in such interpretation the deviations from the pure octahedral symmetry of the NiO_6^{10-} cluster are supposed to be negligible [3]; however, at the same time, all transitions between the $^3A_{2g}$ (T_2) and A_2, E, T_1, T_2 states are allowed in the magnetic dipole approximation and it is not clear why two of them are not detected in the experimental spectra [9].

Another explanation was advanced in Ref. [15]. An experimental basis for it is that only two peaks are seen in the spectral region of the $^3A_{2g}$–$^3T_{2g}$ absorption transition [7,16,17], which allowed to propose a hypothesis that the nickel ions in MgO are displaced from the center of the oxygen octahedron due to the structural relaxation after doping. Such a situation was reported to take place in many impurity centers formed by the transition metal ions and Ni^{2+} ions in particular, like in similar crystals of CaO, SrO and BaO [18–23]. The distortion of the oxygen octahedron then would produce the low-symmetry (trigonal) component of CF, which would split the $^3T_{2g}$ electronic state into two sublevels. However, the latter hypothesis has been considered so far only qualitatively, without being proved by any theoretical calculations.

* Corresponding author. Tel.: +372 7374751; fax: +372 7383033.
E-mail address: brik@fi.tartu.ee (M.G. Brik).

0022-2313/$ - see front matter © 2012 Elsevier B.V. All rights reserved.
http://dx.doi.org/10.1016/j.jlumin.2012.10.026

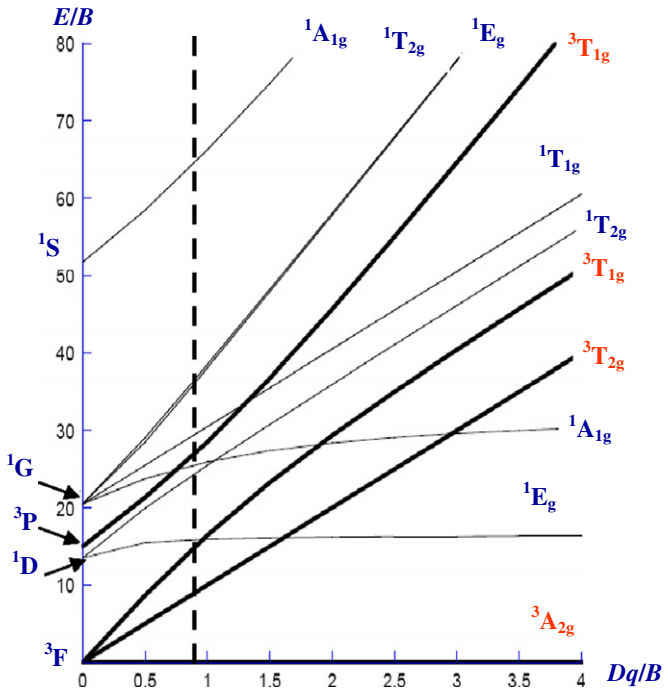

Fig. 1. Tanabe–Sugano diagram for the $3d^8$ electron configuration in the octahedral CF. The spin-triplet and spin-singlet states are shown by the thick and thin lines, respectively; the vertical dashed line indicates the CF strength for MgO:Ni^{2+}.

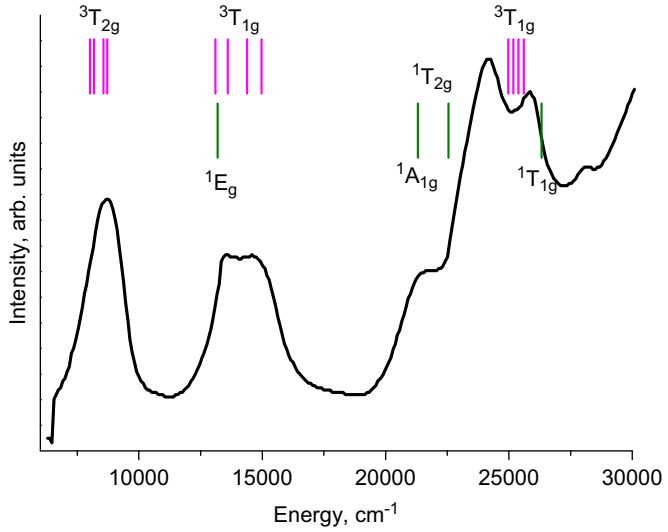

Fig. 2. Experimental room-temperature absorption spectra of Ni^{2+} in MgO [14,42]. The calculated Ni^{2+} energy levels for the O_h site positions are shown by the vertical lines.

We also mention that an idea of the *local* low-symmetry CF existing around divalent nickel ions in magnesium oxide was suggested in some earlier works [24,25]; such an idea was based on peculiar features (widths, shapes and dependence of the line width on the magnetic field orientation relative to the crystal axes) of the electron paramagnetic resonance (EPR) spectra of MgO:Ni^{2+}. Nevertheless, such a local CF was assumed to produce inhomogeneous broadening of the EPR lines only, without leading to the splitting of the orbital triplet states.

The main aim of the present paper was set to perform consistent CF calculations of the Ni^{2+} energy levels in MgO assuming the ideal O_h symmetry with taking into account SO interaction; we have also tested the idea of the off-center displacements of nickel ions. All calculated results were compared to the corresponding experimental optical spectra and (if necessary) to the EPR experimental data. In the performed calculations the use was made of the exchange charge model (ECM) [26] of CF. This model allows for direct explicit calculations of the crystal field parameters (CFP) from the crystal structure with subsequent diagonalization of the impurity ion CF Hamiltonian and comparison of the calculated eigenvalues to the experimental absorption spectra. In this way, one can model straightforwardly all low-symmetry CF effects and follow their manifestations in the optical absorption spectra by assigning the fine structure of the experimental absorption bands to the calculated energy levels.

It is worthwhile noting that the nickel ions in MgO even at rather low concentrations (between 2 and 5%) tend to form the exchange–correlated pairs [7,12], which may lead to observations of additional lines in the optical spectra. The Ni–Ni pair's formation is enhanced at higher Ni concentrations (up to 10%); for such samples the number of the observed absorption peaks is large, which makes interpretation of the experimental results ambiguous. However, at lower concentrations (about 1%), when the Ni^{2+} ions are located at a rather large distance from each other in the MgO crystal lattice, these additional lines disappear. Therefore, for a meaningful analysis of the CF effects without Ni–Ni exchange magnetic interaction, only low-concentrated MgO:Ni^{2+} crystals should be used, as has been done in the present paper.

The paper is organized as follows: in the next section we describe briefly the model used for the calculations, then we proceed by presenting the main results accompanied by their discussion. The paper is concluded with a short summary.

2. Method of calculations

The energy levels of impurity ions with an unfilled d-shell (in our case, Ni^{2+} ion with its $3d^8$ electron configuration) in a CF of arbitrary symmetry can be represented by the eigenvalues of the following CF Hamiltonian [26]:

$$H = \sum_{p=2,4} \sum_{k=-p}^{p} B_p^k O_p^k, \tag{1}$$

where O_p^k are the linear combinations of the spherical operators acting on the angular parts of the impurity ion's wave functions (exact definition of the operators used in the ECM can be found in Ref. [26]), and B_p^k are the CFP, which can be calculated from the available crystal structure data. They include all the structural and geometrical information about the impurity center and reflect arrangement of the host lattice ions around the impurity site. The Hamiltonian (1) is defined in the effective space spanned by all wave functions of the free ion's LS terms, which are due to the Coulomb interaction between electrons of an impurity ion. In the case of Ni^{2+} ions there are five such terms: ^3F (the ground state), ^3P, ^1D, ^1G and ^1S. In the ECM framework, the CFP are represented as a sum of two contributions [26]:

$$B_p^k = B_{p,q}^k + B_{p,S}^k \tag{2}$$

which, in their turn, are calculated as follows:

$$B_{p,q}^k = -K_p^k e^2 \langle r^p \rangle \sum_i q_i \frac{V_p^k(\theta_i,\phi_i)}{R_i^{p+1}}, \tag{3}$$

$$B_{p,S}^k = K_p^k e^2 \frac{2(2p+1)}{5} \sum_i \left(G_s S(s)_i^2 + G_\sigma S(\sigma)_i^2 + \gamma_p G_\pi S(\pi)_i^2 \right) \frac{V_p^k(\theta_i,\phi_i)}{R_i} \tag{4}$$

Eq. (3) describes the point charge contribution to the CFP, which arises from the electrostatic interaction between the central ion and the lattice ions enumerated by index i with charges q_i and spherical coordinates, R_i, θ_i, ϕ_i(with the reference system centered at the impurity ion itself). The averaged values$\langle r^p\rangle$, where r is the radial coordinate of the d electrons of the considered impurity ion, can be obtained either from the literature or calculated numerically, using the radial parts of the corresponding ion's wave functions. The values of the numerical factorsK_p^k, γ_p, the expressions for the polynomials V_p^k and the definitions of the operators O_p^k can all be found in Ref. [26] and thus are not shown here for the sake of brevity. Eq. (4) determines the so called exchange charge contribution to the CFP; it is proportional to the overlap between the wave functions of the central ion and ligands and thus includes all covalent effects. The $S(s)$, $S(\sigma)$, $S(\pi)$entries correspond to the overlap integrals between the d-functions of the central ion and p- and s-functions of the ligands: $S(s)=\langle d0|s0\rangle$, $S(\sigma)=\langle d0|p0\rangle$, $S(\pi)=\langle d1|p1\rangle$. The G_s, G_σ, G_π coefficients are dimensionless adjustable parameters of the model, whose values are determined from the positions of the first three absorption bands in the experimental spectrum. They can be approximated to a single value, i.e.$G_s=G_\sigma=G_\pi=G$, which then can be estimated from one absorption band only (the lowest in energy). This is usually a reasonable approximation [26].

The main advantages of the ECM are the following: i) a small number of fitting parameters, ii) opportunity to calculate the CFP and energy levels of impurities in crystals without invoking any assumptions about the impurity center symmetry, but by using only the crystal structure data, and iii) the possibility to treat the covalent effects quantitatively (by calculating the overlap integrals).

The ECM has been successfully applied for the calculations of energy level of rare earth ions [26–28] and transition metal ions [29–36], so the validity of its application for MgO:Ni^{2+} is fully justified.

3. Samples preparations and spectroscopic measurements

The MgO:Ni^{2+} samples used in the present work were single crystals, grown epitaxially by chemical transport reactions method (the "sandwich" technique) using HCl gas from polycrystalline solid solutions on freshly cut and polished single-crystal MgO (100) as substrates. Polycrystalline solid solutions were prepared using ceramic technology from the appropriate amounts of aqueous solutions of $Mg(NO_3)_2\cdot 6H_2O$ and $Ni(NO_3)_2\cdot 6H_2O$ salts, which were mixed and slowly evaporated with a subsequent heating up to 500–600 °C to remove completely NO_2. The obtained polycrystalline solid solutions were pressed and annealed for 100 h at 1200 °C in the air and rapidly cooled down to room-temperature. The MgO-Ni^{2+} single-crystals obtained in this way have green color and retain orientation of the MgO substrate.

The optical absorption spectra were recorded using the double beam system with a single monochromator Jasco UV/VIS/NIR spectrophotometer (Model V-570, wavelength range 190–2500 nm) with a deuterium lamp (190–350 nm) and a halogen lamp (330–2500 nm) used as excitation sources. The PbS photoconductive cell was used as a detector. A liquid helium cryostat was used to control the temperature of the samples down to 5 K with an accuracy ± 1 K.

4. Results of calculations and discussion

The crystal structure data from Ref. [37] were used to calculate the CFP values. According to Ref. [37], MgO is crystallized in the cubic structure, space group Fm3m (No. 225), lattice constant 4.211 Å. In this structure, each ion has six nearest neighbors, which form an ideal octahedron. To ensure convergence of the crystal lattice sums in Eq. (3), a large cluster consisting of 24,390 ions was considered, which accounts for contribution of ions located at the distances up to 51 Å from Ni^{2+} ion.

The Ni^{2+}–O^{2-} overlap integrals needed for calculations of the exchange charge contribution to the CFP were calculated numerically using the radial wave functions of the Ni^{2+} and O^{2-} ions from Refs. [38,39]. For further convenience, they were approximated by the following exponential functions of the interionic separation R (expressed in a.u.):

$$S_s=\langle d0|s0\rangle=-0.99799\exp(-0.73145R),$$
$$S_\sigma=\langle d0|p0\rangle=0.84696\exp(-0.68325R),$$
$$S_\pi=\langle d1|p1\rangle=1.13280\exp(-0.86486R). \quad (5)$$

We have considered the Ni^{2+} ions at the central position in the oxygen octahedron with the O_h symmetry. The CFP in this case (Table 1) were calculated in the crystallographic system of coordinates. Only two CFP - namely, B_4^0, B_4^4 - are not zero; they are related to each other by the following ratio $B_4^4=5B_4^0$ (the Stevens normalization).

The point and exchange charge contributions are given separately, to highlight importance of the exchange and covalent effects in formation of the Ni^{2+} energy levels in MgO. As seen from Table 1, for the B_4^0, B_4^4 parameters the former constitutes only about 25% from the total value. Considerable covalent effects existing between the Ni^{2+} and O^{2-} ions in MgO (as confirmed by the present calculations) were also emphasized by Low [40,41].

The CF Hamiltonian (1) with CFP from Table 1 was diagonalized in the space spanned by 45 (if the SO interaction was accounted for) wave functions of all five LS terms (^3F, ^3P, ^1D, ^1G, ^1S) of the $3d^8$ electron configuration. The ECM parameter was determined using the experimental data on the splitting of the ground ^3F term, in particular, position of the first absorption band [14,42]; its value was found to be 4.201. The chosen values of the Racah parameters B and C, which provide the best agreement with experimental data, are also given in Table 1. The CF Hamiltonian was then diagonalized; the calculated nickel energy levels are collected in Table 2. All Ni^{2+} energy levels are assigned using the O_h point group irreducible representations and parent LS terms of a free ion. The calculated energy levels are in good agreement with the experimental findings. The energy levels of such cubic center (Table 2) were calculated taking into account SO interaction with the value of the SO interaction constant ζ=-620 cm^{-1}. These calculated energy levels are also shown in Fig. 2. As seen from Fig. 2, the O_h symmetry approximation with SO interaction can reproduce well the location of the $^3T_{2g}$, $^3T_{1g}$ (^3F) states, but fails to describe the structure of the $^3T_{1g}$ (^3P) absorption band. We also note that only two (lowest in energy) out of four SO components of the $^3T_{2g}$ state were experimentally detected [3,9], so the width of the $^3T_{2g}$ band can be explained in this case only by electron-vibrational interaction.

The experimental room-temperature absorption spectrum of Ni^{2+} in MgO is shown in Fig. 2. As mentioned in the introduction,

Table 1
Crystal field parameters (in Stevens normalization, cm^{-1}) for Ni^{2+} in MgO. G=4.201 is the dimensionless ECM parameter; Racah parameters B=935 cm^{-1} and C=3330 cm^{-1}.

	O_h symmetry		
	$B_{p,q}^k$	$B_{p,S}^k$	B_p^k
B_4^0	579.5	1598.0	2177.5
B_4^4	2897.5	7990.0	10887.5

Table 2
Calculated and experimental energy levels (in cm^{-1}) for Ni^{2+} in MgO. The symbols in parenthesis are the irreducible representations of the SO split levels in the corresponding point group indicated in the column heading.

Energy levels	Calculated (this work, O_h with SO)	Experiment (this work)
(O_h group notation and "parent" LS term)		
$^3A_{2g}$ (^3F)	0 (T_2)	
$^3T_{2g}$ (^3F)	8009 (E), 8173 (T_1), 8556 (T_2), 8711 (A_2)	8005 8182
$^3T_{1g}$ (^3F)	13103 (A_1), 13604 (T_1), 14380 (T_2), 14972 (E)	13400 14500
^1E_g (^1D)	13196 (E)	13535
$^1T_{2g}$ (^1D)	21304 (T_2)	21300
$^1A_{1g}$ (^1G)	22556 (A_1)	
$^3T_{1g}$ (^3P)	24971 (E), 25183 (T_2), 25392 (T_1), 25602 (A_1)	24000 25600
$^1T_{1g}$ (^1G)	26327 (T_1)	
^1E_g (^1G)	32394 (E)	
$^1T_{2g}$ (^1G)	32830 (T_2)	
$^1A_{1g}$ (^1S)	56114 (A_1)	

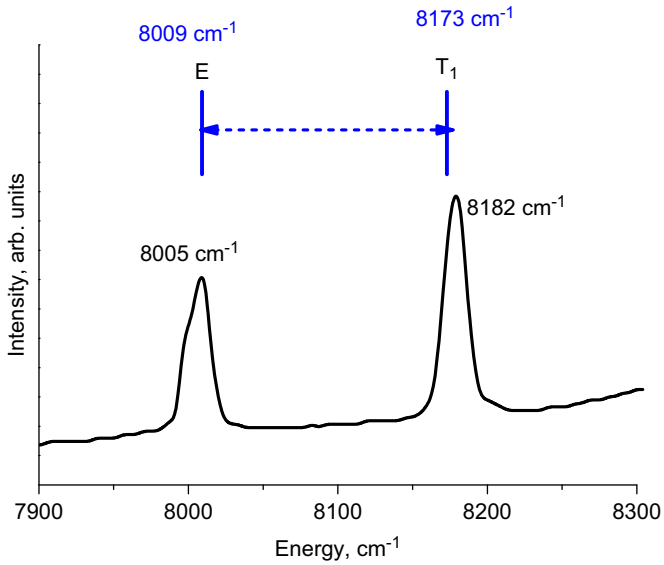

Fig. 3. Structure of the low-temperature absorption band corresponding to the $^3A_{2g}$–$^3T_{2g}$ transition. Two vertical lines show two lowest calculated SO components of the $^3T_{2g}$ state.

the three spin-allowed transitions to the $^3T_{2g}(^3F)$, $^3T_{1g}(^3F)$ and $^3T_{1g}(^3P)$ excited states determine its overall appearance. A structure of the absorption peaks is due to the combination of two reasons: i) SO splitting of the spin-triplet states; ii) weak spin-forbidden transitions superimposed onto the spin-allowed ones.

The structure of the $^3T_{1g}(^3F)$ absorption band is also affected by the presence of the spin-singlet ^1E_g at 13,536 cm^{-1}. A low-energy shoulder (at about 22,000 cm^{-1}) of the $^3T_{1g}(^3P)$ absorption band is due to the spin-forbidden transitions from the ground state $^3A_{2g}$ to the spin-singlet states $^1A_{1g}$ and $^1T_{2g}$.

Coming back to the fine structure of the first excited state, Fig. 3 illustrates the agreement between the two lowest components of the $^3T_{2g}$ state (split by the SO interaction) and experimental absorption spectrum. Two experimentally observed absorption peaks at 8005 cm^{-1} and 8182 cm^{-1} are perfectly matched by the two calculated energy levels at 8009 cm^{-1} and 8173 cm^{-1}, produced by the SO splitting.

The energy separation between the $^3A_{2g}$ and $^3T_{2g}$ states of the $3d^2/3d^8$ electron configurations is equal to the CF strength $10Dq$ [44]. Taking the value of Dq as 810 cm^{-1} (rounding off the weighted average energy of the $^3A_1$ ($^3T_{2g}$) and ^3E ($^3T_{2g}$) states), we get the Dq/B ratio as 0.87. It is shown by a vertical dashed line in Fig. 1, which corresponds to the weak CF case in MgO:Ni^{2+}.

We also calculated the energy levels of the Ni^{2+} ions assuming the off-center displacement of the Ni^{2+} along the (111) direction with the resulting trigonal symmetry around impurity ions. The value of such a displacement, which allowed for a proper reproduction of the $^3T_{2g}$ energy levels, was 0.2 Å. The obtained value of the Ni^{2+} displacement (0.2 Å) can be favorably compared to the previously reported in the literature off-center displacements of the Ni^{2+} ions in similar crystals of SrO (0.26 Å) [21] and Fe^{3+} in SrO (0.22 Å) [46]. However, with such a displacement in the MgO:Ni^{2+} system the zero-field splitting of the ground $^3A_{2g}$ state would be 4 cm^{-1}; such a result contradicts, however, to the absence of the ground state zero-field splitting in the EPR measurements [1,43,45].

A few more comments on the considered system of MgO:Ni^{2+} seem to be appropriate at this point. The cubic symmetry of the host and its seeming simplicity can mask quite many phenomena, which can be uncovered by scrutinizing the optical spectra and structural relaxation effects with simultaneous elaborating of the existing models with an attempt of improved description of the experimental data. It is clear that the perfectly octahedral CF around nickel ions in MgO does not allow for a unique and adequate interpretation of the EPR and optical experimental data simultaneously. We believe that additional thorough studies - both experimental and theoretical - are required to determine exactly the structure of the NiO_6^{10-} cluster in MgO and find more decisive arguments in favor of either octahedral or trigonal CF acting upon the nickel ions in magnesium oxide.

Another possible phenomenon, which cannot be ruled out and which is known to play an important role in many transition-metals bearing crystals, is the Jahn–Teller effect, which also can lead to the oxygen octahedron deformations in MgO, and quenching of the SO splitting. In this connection we mention here some earlier and very recent publications [47,48] devoted to the optical and EPR spectra of an immediate successor of nickel in the periodic table - copper. The divalent copper has a close to divalent nickel ionic radius, identical charge, but different electronic configuration ($3d^9$). The tetragonal distortions of the CuO_6^{10-} cluster in CaO and MgO [47] were analyzed in terms of the Jahn–Teller effect to account for the particular features of the corresponding Cu^{2+} EPR spectra. Ab initio calculations of the tunneling splitting and Jahn–Teller effect for the CaO:Cu^{2+} and MgO:Cu^{2+} systems were performed recently [48], thus showing unquestionable importance of the first principles calculations for an analysis of the structural properties of impurity centers in crystals. Also Jahn–Teller effect was considered as a reason for lowering the symmetry of the impurity centers formed by Ag^{2+} ion ($3d^9$ configuration) in SrO, CaO, and MgO [49].

It has been also shown in Ref. [50] that in lattices with fluorite structure the off-center displacement of an impurity ion can be observed in soft lattices, e.g. in $SrCl_2$ lattice both Cu^{2+} and Ag^{2+} impurities are subject to such a displacement, while in SrF_2 only Cu^{2+} undergoes a small off-centre shift, and Cu^{2+} and Ag^{2+} in CaF_2 remain exactly at the substituted Ca^{2+} site.

These comments show how complicated a simple cubic crystal can be, especially when several approaches to the description of its optical properties can produce similar or comparable results.

5. Conclusions

In the present paper we used the exchange charge model of crystal field to calculate the energy levels of Ni^{2+} ions in MgO.

Assuming the Ni^{2+} ions to be situated at the central position of the oxygen cluster we calculated their energy levels with taking into account the spin-orbit interaction. We also considered possible off-center displacements of the nickel ions along the (111) direction; however, in this case a large value of the calculated zero-field splitting ($4\,cm^{-1}$) contradicts to the experimental data, which reported absence of such a splitting in the $^3A_{2g}$ ground state.

It is hoped that the questions raised in the present work would induce researchers to take a closer look at the MgO:Ni^{2+} system with an aim of clarifying the structure and geometry of nearest surrounding of the nickel ions. To this end, some additional studies - both experimental (EPR, X-ray and optical absorption spectroscopy) and theoretical (including the ab initio methods) - of MgO:Ni^{2+} may be needed.

Acknowledgment

The authors from Tartu acknowledge the European Union through the European Regional Development Fund (Centre of Excellence "Mesosystems: Theory and Applications", TK114). The author from Riga was supported by the grant of the Latvian Government (No 09.1580).

References

[1] R. Pappalardo, D.L. Wood, R.C. Linares Jr., J. Chem. Phys. 35 (1961) 1460.
[2] J.E. Ralph, M.G. Townsend, J. Chem. Phys. 48 (1968) 149.
[3] N.B. Manson, Phys. Rev. B 4 (1971) 2645.
[4] N.B. Manson, Phys. Rev. B 4 (1971) 2656.
[5] B.D. Bird, G.A. Osborne, P.J. Stephens, Phys. Rev. B 5 (1972) 1800.
[6] J.E. Ralph, M.G. Townsend, J. Phys. C: Solid State Phys. 3 (1970) 8.
[7] G.A. Grinvald, N.A. Mironova, Phys. Stat. Sol. B 99 (1980) K101.
[8] W.C. Zheng, Phys. Rev. B 40 (1989) 7292.
[9] C. Campochiaro, D.S. McClure, P. Rabinowitz, S. Dougal, Phys. Rev. B 43 (1991) 14.
[10] R. Llusar, M. Casarrubios, Z. Barandiarán, L. Seijo, J. Chem. Phys. 105 (1996) 5321.
[11] D.P. Ma, N. Ma, X.D. Ma, H.M. Zhang, J. Phys. Chem. Solids 59 (1998) 1211.
[12] X.Y. Kuang, K.W. Zhou, Physica B 305 (2001) 169.
[13] C. Rudowicz, Y.Y. Yeung, Z.Y. Yang, J. Qin, J. Phys.: Condens. Matter 14 (2002) 5619.
[14] N. Mironova-Ulmane, V. Skvortsova, A. Kuzmin, U. Ulmanis, I. Sildos, E. Cazzanelli, G. Mariotto, Phys. Solid State 47 (2005) 1516.
[15] N. Mironova, A. Kuzmin, J. Purans, A. Rodionov, SPIE Proc. 2706 (1995) 168.
[16] G.A. Grinvald, N.A. Mironova., Izv. Akad. Nauk LatvSSR. Ser. Fiz. Tech. Nauk 4 (1978) 79.
[17] N. Mironova, V. Skvortsova, A. Kuzmin, J. Purans., J. Lumin. 72–74 (1997) 231.
[18] N.B. Manson, A. Edgar, Semiconductors and Insulators 3 (1978) 209.
[19] V.A. Krylov, W. Ulrici, L.S. Sochava, Phys. Stat. Sol. A 56 (1979) 615.
[20] A. Edgar, Y. Haider, J. Magn. Magn. Mater. 15 (1980) 745.
[21] M.J.L. Sangster, A.M. Stoneham, Phil. Mag. B 43 (1981) 597.
[22] T.J. Hosea, N.B. Manson, Sol. State Commun. 38 (1981) 469.
[23] G.D. Lu, H.W. Zhang, X.L. Tang, Z.Y. Zhong, L. Peng, Chin. Phys. Lett. 26 (2009) 086103.
[24] J.W. Orton, P. Auzins, J.E. Wertz, Phys. Rev. 119 (1960) 1691.
[25] J.W. Orton, P. Auzins, J.H.E. Griffiths, J.E. Wertz, Proc. Phys. Soc. 78 (1961) 554.
[26] B.Z. Malkin, in: A.A. Kaplyanskii, B.M. Macfarlane (Eds.), Spectroscopy of solids containing rare-earth ions, North-Holland, Amsterdam, 1987, pp. 13–50.
[27] M. Kirm, G. Stryganyuk, S. Vielhauer, G. Zimmerer, V.N. Makhov, B.Z. Malkin, O.V. Solovyev, R.Y. Abdulsabirov, S.L. Korableva, Phys. Rev. B 75 (2007) 075111.
[28] B.Z. Malkin, T.T.A. Lummen, P.H.M. van Loosdrecht, G. Dhalenne, A.R. Zakirov, J. Phys.: Condens. Matter 22 (2010) 276003.
[29] C. Jousseaume, D. Vivien, A. Kahn-Harari, B.Z. Malkin, Opt. Mater. 24 (2003) 143.
[30] M. Vaida, C.N. Avram, Acta Phys. Polonica A 116 (2009) 541.
[31] M.L. Stanciu, M.G. Ciresan, N.M. Avram, Acta Phys. Polonica A 116 (2009) 544.
[32] N.M. Avram, M.G. Brik, I.V. Kityk, Opt. Mater. 32 (2010) 1668.
[33] M.G. Brik, C.N. Avram, J. Lumin. 131 (2011) 2642.
[34] A.M. Srivastava, M.G. Brik, J. Lumin. 132 (2012) 579.
[35] M. Vaida, Phys. Scr. T149 (2012) 014059.
[36] Q. Wei, L.-X. Guo, B. Wei, Z.-Y. Yang, Opt. Mater. 34 (2012) 1092.
[37] L.S. Dubrovinsky, S.K. Saxena, Phys. Chem. Miner. 24 (1997) 547.
[38] E. Clementi, C. Roetti, Atom Data Nucl. Data Tables 14 (1974) 177.
[39] M.V. Eremin, in: Spectroscopy of Crystals (in Russian), Moscow, 1989, pp. 30–44.
[40] W. Low, Phys. Rev. 105 (1957) 793.
[41] W. Low, Phys. Rev. 105 (1957) 801.
[42] N.A. Mironova, U.A. Ulmanis, Radiation Defects and Metal Ions of Iron Group in Oxides, Zinatne, Riga, 1988.
[43] W.L. Feng, X.M. Li, W.J. Yang, C.Y. Tao, Y.L. Yang, Optik 122 (2011) 1512.
[44] S. Sugano, Y. Tanabe, H. Kamimura, Multiplets of Transition-Metal Ions in Crystals, Academic, New York, 1970.
[45] Z.-H. Zhang, S.-Y. Wu, P. Xu, L.-L. Li, Braz. J. Phys. 40 (2010) 361.
[46] A.F.M.Y. Heider, A. Edgar, J. Phys. C: Solid State Phys. 15 (1982) L41.
[47] R.W. Reynolds, L.A. Boatner, M.M. Abraham, Y. Chen, Phys. Rev. B 10 (1974) 3802.
[48] P. García-Fernández, A. Tueba, M.T. Barriuso, J.A. Aramburu, M. Moreno, Phys. Rev. Lett. 104 (2010) 035901.
[49] L.A. Boatner, R.W. Reynolds, M.M. Abraham, Y. Chen, Phys. Rev. Lett. 31 (1973) 7.
[50] M. Moreno, M.T. Barriuso, J.A. Aramburu, P. García-Fernández, J.M. García-Lastra, J. Phys.: Condens. Matter 18 (2006) R315.